Soft Matter

Cite this: *Soft Matter*, 2012, **8**, 9086

www.rsc.org/softmatter

PAPER

Wrinkling and strain localizations in polymer thin films†

Yuri Ebata,[a] Andrew B. Croll[b] and Alfred J. Crosby*[a]

Received 12th April 2012, Accepted 12th July 2012
DOI: 10.1039/c2sm25859e

Wrinkles and strain localized features are observed in many natural systems and are useful surface patterns for a wide range of applications, including optical gratings and microfluidic devices. However, the transition from sinusoidal wrinkles to more complex strain localized features, such as delaminations or folds, is not well understood. In this paper, we investigate the onset of wrinkling and strain localizations in a model system of a glassy polymer film attached to a surface of an elastomeric substrate. We show that careful measurement of feature amplitude as a function of applied strain allows not only the determination of wrinkle, fold, or delamination onset but also allows clear distinction between each type of feature. We observe that amplitude increases discontinuously as delamination occurs; whereas, the amplitude for a fold deviates gradually compared to the amplitude for a nearby wrinkle as a function of applied strain. The folds observed in these experiments have an outward morphology from the surface, in contrast to folds that form into the plane for a film floating on a liquid substrate. A deformation mode map is presented, where the measured critical strain for localization is compared for films with thickness ranging from 5 nm to 180 nm.

1 Introduction

Wrinkling is a phenomenon commonly observed in everyday life, such as in ageing human skin or ripening fruits, and has been studied extensively both theoretically[1–4] and experimentally.[5–10] Wrinkling is a low-strain buckling behavior that occurs when an in-plane compressive strain exceeds a critical value for a thin rigid film attached to a soft underlying substrate, thus causing the composite surface to deform out of plane in a periodic manner.[11] In contrast to the periodic sinusoidal deformation of wrinkling, strain localization, such as folding or delamination, may occur as an applied compressive strain increases beyond a critical value. These strain localizations occur due to an instability associated with a geometric non-linearity.[12] In essence, localization of applied global strains necessitates the growth of a particular wrinkle in comparison to its neighbours. This transition from wrinkles to localized features is crucial for morphogenesis of many biological systems, such as ciliary folds in embryonic development,[13] and has also raised interest among researchers for technological applications, such as microelectronics[14] and microfluidics.[15] However, a fundamental understanding of the transition from wrinkling to strain localization is still lacking.

Recently, several researchers have investigated the wrinkling and folding of a thin film floating on a fluid surface.[12,16–18] Under uniaxial compression, wrinkling amplitude scaled as the square root of applied strain until a fold occurred. As the wrinkle transitioned to a fold, its amplitude increased linearly; whereas, adjacent wrinkle amplitudes decayed. These important experimental results provide a starting point towards understanding the relationship between wrinkling and strain localization, but the geometry, boundary conditions, and material systems were not relevant for many technologies where solid–solid interfaces are used. These differences are likely to play a critical role in the transition from wrinkling to folding. In this paper, we investigate the differences among wrinkling, folding, and delamination of a glassy polymer film attached to an elastomeric substrate. Using measured differences in amplitude, we examine how material parameters control the critical strains for the transition from wrinkling to strain localization.

2 Experimental

Substrate preparation

Crosslinked polydimethylsiloxane (PDMS) was prepared by mixing Dow Corning Sylgard™184 pre-polymer with the cross-linker in 20 : 1 and 10 : 1 ratios. The mixture was then degassed for 30 minutes, poured into a 10 cm by 10 cm polystyrene petri dish with a thickness of 3–5 mm, and cured at 70 °C for 20 hours. After cooling, the PDMS substrate was cut into rectangular sections of 6 cm × 1 cm × 4 mm. The elastic modulus (E_s) of these substrates was measured using a JKR contact mechanics technique with a 5 mm diameter spherical glass probe.[7] The

[a]*Department of Polymer Science and Engineering, University of Massachusetts, 120 Governors Drive, Amherst, MA, 01003, USA. E-mail: crosby@mail.pse.umass.edu*
[b]*Department of Physics, North Dakota State University, 1211 Albrecht Blvd, Fargo, ND, 58108, USA. E-mail: andrew.croll@NDSU.edu*
† Electronic supplementary information (ESI) available. See DOI: 10.1039/c2sm25859e

average E_s of substrates prepared from 20 : 1 and 10 : 1 formulations was 0.75 ± 0.05 MPa and 1.95 ± 0.3 MPa, respectively.

Film preparation

Atactic polystyrene (PS) with $M_w \sim 115$ kg mol^{-1} and ~1050 kg mol^{-1} was used as received from Polymer Source, Inc. PS solutions in toluene were prepared at various concentrations and spun cast onto a clean sheet of mica. The thickness of PS film was varied from 5 nm to 180 nm, as measured by a Filmetrics F20 interferometer, a Zygo Newview 7300 optical profilometer, and a Veeco Dimension 3100 atomic force microscope.

Mechanical deformation experiments

The PDMS substrates were stretched by ~10% on a custom-built uniaxial strain stage manually in the direction of the substrate's long axis. A PS film was floated on water, transferred to a circular washer, and then subsequently transferred to the pre-stretched PDMS substrate. As the global strain (ε, distance compressed divided by the original length) was released, surface deformations, including wrinkles, folds, and delaminations, were observed using an optical microscope, an optical profilometer, and an atomic force microscope. The global strain rate was approximately 0.0025 s^{-1}. Optical microscopy and optical profilometry measurements of surface deformations were made with 60 s of reaching specified applied strains.

3 Results

We observed different surface deformations, shown schematically and in representative optical micrographs in Fig. 1, as global compressive strains were applied to the PS films attached to the PDMS substrates. In general, wrinkling is a sinusoidal and uniform deformation; whereas, folding and delamination have a localized increase in amplitude. Folds generally formed in a staggered manner. Delaminations propagated across the surface. Delamination, in general, can be differentiated from folding in optical images by the interference pattern caused by the air gap between the film and substrate, but for localizations with dimensions smaller than optical resolution the differences in amplitude and curvature shown in Fig. 2 must be used for differentiation. Also, we did not observe any sliding of the film with respect to the substrate in our experimental system at macroscopic length scales.

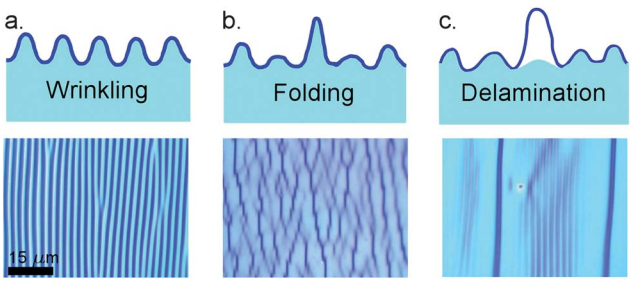

Fig. 1 Schematic and optical microscope images of (a) wrinkling, (b) folding, and (c) delamination. The scale bar is same for all images, and the film thickness and applied global strain are (a) $t = 60$ nm, $\varepsilon = 0.02$, (b) $t = 25$ nm, $\varepsilon = 0.04$, (c) $t = 60$ nm, $\varepsilon = 0.05$.

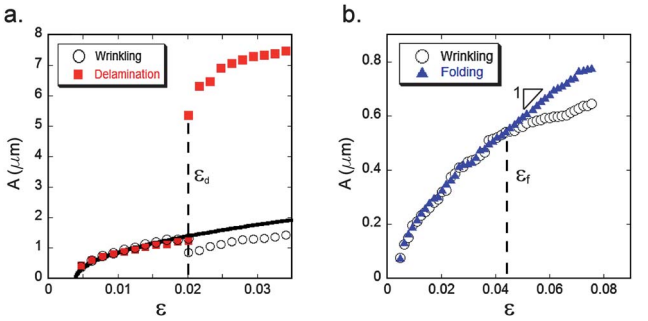

Fig. 2 Amplitude as a function of applied global strain for (a) delamination and (b) fold. The amplitude of a nearby wrinkle is shown in both (a) and (b) in open circles. The solid black line in (a) shows the square root scaling for wrinkling predicted by eqn (2). The experiments shown were (a) 230 nm thick PS film on 20 : 1 PDMS and (b) 70 nm thick PS film on 20 : 1 PDMS, respectively.

The critical global strain for each deformation is defined as ε_w for wrinkling, ε_f for folding, and ε_d for delamination. Wrinkling has a well-defined wavelength, λ, which depends on film thickness t, the elastic modulus of the film E_f, the elastic modulus of the substrate E_s, and scales as:[19]

$$\lambda \sim t\left(\frac{E_f}{3E_s}\right)^{1/3}. \quad (1)$$

In our material system, it was confirmed that the wrinkling wavelength follows the classical scaling shown in eqn (1) [see ESI†]. To investigate the differences quantitatively between the wrinkles and the strain localized features, the amplitude of the buckled structures was quantified as a function of the compressive global strain (Fig. 2). Although wrinkle wavelength is known to be weakly dependent upon strain,[20] we do not resolve these differences with our chosen methods [fast Fourier transform of optical images captured as a function of applied strain are provided in ESI†]. In this paper, amplitude is defined as the distance between the peak and the valley of the buckled features. Fig. 2 shows the amplitude growth of a single wrinkle transitioning into a strain localized feature as global strain is applied, and is compared to the amplitude growth of a nearby wrinkle which is not observed to localize on the same sample.

The amplitude of a wrinkle is known to scale as:[19]

$$\frac{A_w}{\lambda} \sim \varepsilon^{1/2}, \quad (2)$$

where ε is the applied global strain and A_w is the amplitude of wrinkling. For low global strains, the amplitude of all topographic features followed the wrinkling behavior described in eqn (2). When delamination occurred, the amplitude of a local feature increased discontinuously at ε_d and continued to increase with global strain (Fig. 2a). The wrinkle amplitude nearby the delamination (distance of 3λ away) decreased at the instant delamination occurred, but continued to increase as more strain was applied. For structures which we describe as folds (Fig. 2b), the amplitude slowly deviated from the wrinkling behavior and had a linear relationship with the applied global strain up to a strain of 0.1 (Fig. 2b). This linear relationship is consistent with the observed high strain behavior of a film compressed on a liquid substrate;[16,21] however, important differences are

observed. First, the wrinkling amplitude near the fold (3λ away) did not decay after the fold formation. This observation confirms that the strain released during fold formation is a local event, and the global strain is recovered over a materials-defined length scale associated with the thickness of the film and the elastic modulus mismatch of the film and the substrate. We observe that this distance is on the order of λ, which is consistent with inter-fold length scales recently observed for a thin, glassy block copolymer film placed on an elastomer.[22] A second difference between the folds observed in our experiments and folds on liquid substrates is that multiple folds, not a single fold feature, is observed across the entire sample (Fig. 1b). Again, this observation is consistent with the concept of strain released during folding being local, such that films with lateral dimensions greater than a material-defined size will exhibit multiple folds.

A closer look at the topographic shape of each deformation also highlights key differences compared with features observed in compressed films on liquid surfaces. A cross-section in Fig. 3a, obtained by optical profilometry, shows that the delamination amplitude is very large compared to the amplitude of wrinkling or folding, and that the wrinkling amplitude near a delamination decreases. Wrinkle and fold cross-sections are similar, but folding shows one peak that is slightly larger than other peaks [see ESI† for a cross-section of wrinkles and folds obtained by AFM]. It is important to note here that the folding we observed was always out of the substrate, which contrasts other recent observations for folding films.[21,22] Since the amplitude change for a fold can be slight at the initial onset, the second derivative of amplitude with respect to the distance, or curvature, can highlight the key difference between wrinkling and folding, as shown in Fig. 3b. For sinusoidal wrinkling, the second derivative also is sinusoidal. For folding deformations, the localization feature has a curvature that deviates from a smooth sine wave. A large negative curvature is observed at the peak of the fold, and the difference between the peak and valley of the fold curvature is significantly larger than that of the wrinkle.

In order to study the amplitude progression as a function of applied global strain more statistically, an amplitude histogram as a function of global applied strain is constructed by quantifying the amplitudes of all surface deformations across a representative area of a compressed sample. To collect this data, a program written in Matlab® [provided in ESI†] takes three-dimensional data from optical profilometry measurements and calculates a histogram of the amplitude distribution. Fig. 4 shows a representative amplitude histogram as a sample was compressed. The first column shows the amplitude histogram just after wrinkling occurred on the surface. Since wrinkling is a uniform, sinusoidal deformation, a single peak corresponding to the average wrinkling amplitude is observed. It is important to note that there is polydispersity in the amplitude values even in wrinkling, signifying non-uniformity across the surface. As the system is compressed further, folding occurred, and the amplitude histogram is shown in the second column. After folding, wrinkling features were still dominant as indicated by the larger frequency, but a second peak associated with fold features is observed at higher amplitudes. The wrinkle distribution is also observed to increase in width, which is likely associated with small decreases in wrinkle amplitudes very near to the fold features. After delamination, shown in the third column, the wrinkle amplitude distribution split into multiple peaks, which are associated with the decrease in wrinkle amplitude near delamination features as shown in Fig. 3a.

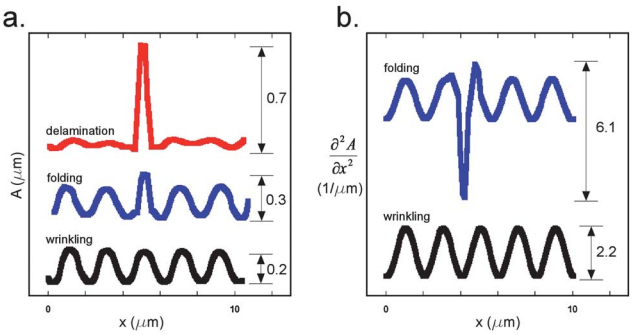

Fig. 3 (a) Cross-section for a typical wrinkle, fold, and delamination, and (b) second derivative of amplitude with respect to position for a wrinkle and fold. The experiment shown was conducted on 60 nm film placed on 20 : 1 PDMS. The data was collected at an applied strain of 0.081.

Using the trademarks described above to distinguish among the buckled structures, we measured the critical strain for the onset of each deformation mechanism as a function of film thickness. Fig. 5 shows our measurement of the critical strain for wrinkling, folding, delamination as a function of film thickness for two different PDMS substrates, with an average elastic moduli of 1.95 MPa (10 : 1) and 0.75 MPa (20 : 1), as well as two different PS materials with molecular weights of ~115 kg mol^{-1} and ~1050 kg mol^{-1}. In the plot, we have combined the experimental data from the two different molecular weights. We define the critical strain, ε_c as:

$$\varepsilon_c = \frac{\Delta_c}{L_0}, \tag{3}$$

where Δ_c is the global deformation distance at which the first deformation mode is observed for a representative area on the sample, and L_0 is the original length of the PDMS sample. For the flat to wrinkle transition, the critical strain is known to scale as:[19]

$$\varepsilon_w = \frac{\Delta_{c,w}}{L_0} \sim \left(E_f^{-2/3} E_s^{2/3}\right), \tag{4}$$

where E_s and E_f is the substrate and film elastic modulus, respectively, and $\Delta_{c,w}$ is the critical deformation distance for wrinkling. Consistent with eqn (3), we find the critical strain for wrinkling is approximately 1% and is independent of film thickness.

Qualitatively, we observed folding in thinner films, and delamination in thicker films. Wrinkling always occurred before localization for film thickness between 5 nm and 180 nm.

4 Discussion

Our results indicate clear differences between wrinkle and strain localized features, providing details of the transition from wrinkling to strain localization in thin films supported by an elastic foundation. In this discussion, we focus on three main topics: (1) the differences of local amplitude measurements

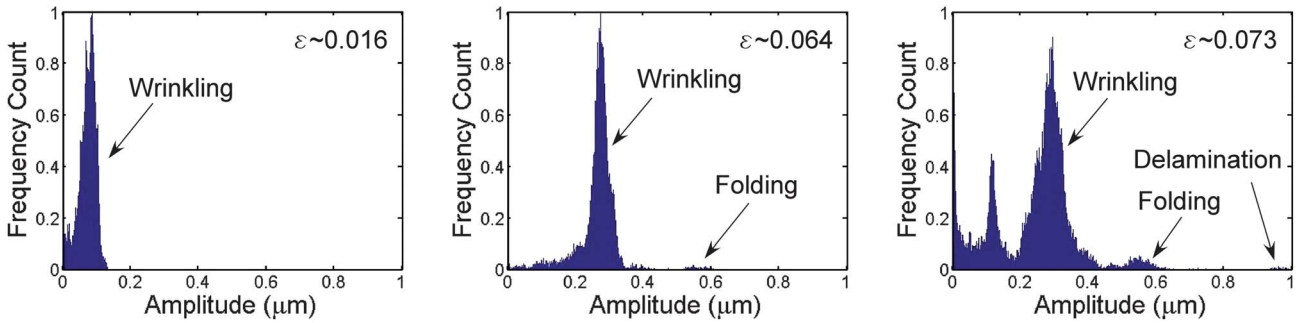

Fig. 4 Amplitude histogram progression of a sample with film thickness of 60 nm placed on top of 20 : 1 PDMS as applied strain is increased: on the *y*-axis is the normalized frequency count, showing relatively how many times each amplitude is observed on a given sample across the optical field. The analyzed image has a dimension of 0.07 mm by 0.05 mm, and the optical profilometer has a lateral resolution of 0.11 μm. The amplitude data was compiled from optical profilometry data using Matlab® program (see ESI† for the code). As the applied strain increased, amplitude peaks for various deformation appeared.

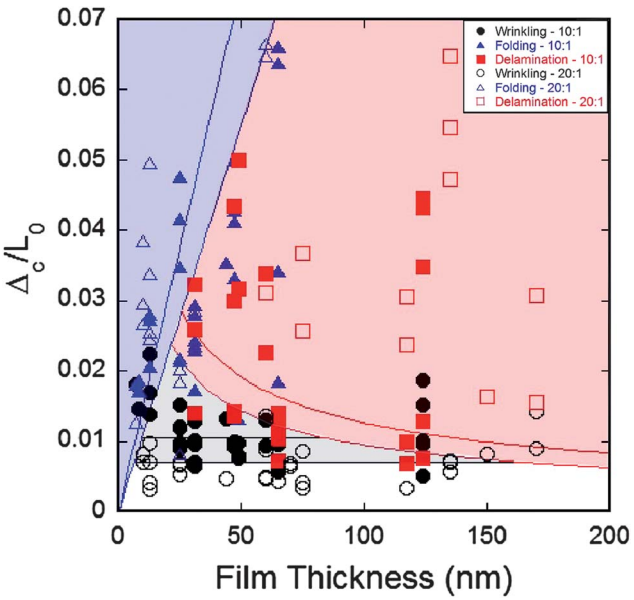

Fig. 5 A deformation mode map showing the critical strains for wrinkling, folding, and delamination with varying film thicknesses. The solid marker represents the experimental data for 10 : 1 PDMS substrates and the open marker represents the experimental data for 20 : 1 PDMS substrates. The experimental data for two different molecular weights (115 kg mol^{-1} and 1050 kg mol^{-1}) has been combined in this plot. The black, circular markers are for the experimental data for wrinkling, the blue, triangular markers are for the experimental data for folding, and the red, square markers are for the experimental data for delamination. The black lines show the wrinkling critical strain based on eqn (4), red lines show the delamination critical strain based on eqn (5), and the blue lines show the folding critical strain based on eqn (6) (see Discussion section). The gray shadow indicates the region where wrinkling is expected, the blue shadow indicates the region where folding is expected, and the pink shadow indicates the region where delamination is expected.

compared to global, statistical amplitude measurements, (2) the critical strain for localization as a function of film thickness, and (3) the observed out-of-substrate growth for folds in our materials system.

Both local and statistical amplitude analysis reveal interesting features of wrinkling, folding, and delamination. Locally, wrinkles behaved sinusoidally with one wavelength and amplitude. Globally, the amplitude histogram showed a distribution of amplitude values centered around an average. While this observation may be intuitive in the context of natural heterogeneities associated with experimental systems, we are not aware of previous reports of a similar quantitative measurement. This distribution is important, especially in the context of strain and stress localization associated with non-linear deformation transitions, such as folding and delamination. Both the local and global analyses showed that the wrinkling amplitude increased smoothly as the applied strain was increased until localization. When folds form, local deformation measurements revealed that the amplitude of the fold increased slightly compared to the amplitude of a nearby wrinkle. From global, statistical measurements, a peak emerged at a higher amplitude compared to the average wrinkle amplitude, showing again that multiple folds occurred across the entire sample. Also, a broadening of wrinkling peak was observed after the fold formation. This broadening is likely associated with a small overall decrease in the amplitude of wrinkles near each of the folds, although this decrease is not always evident locally (Fig. 2). As strain increased, delamination occurred and a distribution in the global statistical measurements was observed at very high amplitudes. Additionally, the wrinkle distribution was observed to split into multiple peaks. It is important to note here that the dominant peak is still the original wrinkling peak, even after the formation of strain localization; however, the peak again broadened, signifying that the wrinkles were less uniform after the formation of delaminations. This non-uniformity was consistent with the observation of local measurements (Fig. 2a), where the wrinkle amplitude decreased near the delamination.

A critical strain map was constructed (Fig. 5) as a function of film thickness, and it was observed generally that folding occurred in thin films and delamination occurred predominantly in thick films. This observation is consistent with the classical description of delamination. When the elastic strain energy released due to the delamination of interfacial area equals or exceeds the critical energy for separating the interface into two surfaces, G_c, then delamination will occur. Following the energy balance approach of Vella, *et al.*[23] [see ESI†], it can be shown that the critical strain for delamination, ε_d scales as:

$$\varepsilon_d \sim \left(\frac{G_c}{E_s t}\right)^{3/5}\left(\frac{E_s}{E_f}\right)^{1/5}. \quad (5)$$

Importantly, eqn (5) shows that the critical strain for delamination is inversely proportional with film thickness to the power of 3/5. We have indicated a line based on this scaling in Fig. 5 to define the region of applied global strains and film thicknesses where delamination is expected, and good agreement is found. Importantly, eqn (5) describes the lowest strain at which a delamination event may occur. We note that this critical strain for delamination diverges as thickness approaches zero, hence a thin film requires a great amount of compression to delaminate.

In thin films, folding occurred before the critical strain for delamination was reached, consistent with the emergence of a different lower energy form of strain localization. The critical strain for folding was considered by Pocivavsek, *et al.*[12] for the uniaxial compression of a film floating on a liquid substrate. Following their energy balance approach, it was shown that the critical strain for folding, ε_f scales as:

$$\varepsilon_f \sim \left(\frac{t}{L}\right)\left(\frac{E_f}{3E_s}\right)^{1/3}, \quad (6)$$

where L is the sample length. Although important differences exist between their material system and ours, we plot this scaling to define the boundary for the region where folding is expected. Although our data is not inconsistent with the linear relationship between critical strain for fold and film thickness, our data for folds of different film thickness was limited and the material system is quite different from a film floating on a liquid substrate. In particular, the PDMS substrate can support a shear stress, thus allowing multiple folds to be observed across the entire surface. Our data cannot confirm that the critical strain for folding is dependent upon film thickness, but we confidently find that folding localizations occur at very small strains that can be nearly equal to the critical strain for wrinkling.

An important difference in our results compared to other folding observations,[12,22] is that folds in our materials grow away from the substrate. This outward growth has also been recently reported by Zhang *et al.*, where they described the formation of "ridges" of a film placed on an elastomer both experimentally and numerically.[24] The material system in their experiment was polydimethylsiloxane (PDMS) with a plasma-treated surface oxide layer. They found that folds grow out of the surface rather than into the surface for a system where the supporting substrate was pre-stretched and released to apply compressive strains to the top surface film. This out-of-plane growth, rather than inward growth, is attributed to the non-linearity of the mechanical properties for the PDMS substrate. Specifically, it was shown through numerical modeling that pre-stretching the elastomeric substrate and subsequently releasing the strain to apply compressive stresses to the top surface film produces a state of stress at the interface of the film and elastomer that energetically favors out-of-plane displacements compared to inward displacements. In our experimental protocol, we pre-stretch the elastomeric substrate and subsequently release the strain to apply compression to the polystyrene film, thus our observation of the out-of-plane fold formation is consistent with the model predictions discussed by Zhang *et al.* Although there is consistency with our experimental observations, key differences exist. For example, as the strain was released, Zhang *et al.* observed fold formation only with a substrate pre-stretch of 1.4 or higher and an onset compressive strain of $\varepsilon_f \sim 0.046$. For our experiments, a pre-stretch between 1.07 and 1.1 was used for all of our samples. This pre-stretch was significantly lower than the critical value reported by Zhang *et al.*[24] Furthermore, regardless of the amount of pre-stretch, we observe ε_f between 0.008 and 0.067 for film thickness of 5 nm to 80 nm. Although this upper-bound of ε_f is similar to the values of Zhang *et al.*, the lower bound is equal or even less than ε_w, implying that folding does not require large strains, in direct contrast to previously published results.[12] Beyond the onset of folds, Zhang *et al.* observed the formation of numerous ridges, similar to our observations; however, they showed numerically that the wrinkling amplitude between ridges should decrease dramatically. As shown in Fig. 2b, we did not observe a decrease in amplitude for wrinkles that are near a fold localization. Rather, we observed a continued increase as the sample was further strained. Although we do not observe any decrease locally, we observe a broadening of the wrinkling amplitude statistical peak (Fig. 4), which suggests that wrinkling amplitude may be decreasing slightly at a distance less than 3λ away.

Although numerical analysis from Zhang *et al.*[24] may describe the general underlying mechanisms for fold formation for a thin elastic film on an elastic substrate, in our experiments the top film is polystyrene, which is known to yield at small strains. If yield or strain softening would occur, it could lead to the initiation of a fold. To consider whether film yielding is responsible for fold formation in our study, we consider the local strain, ε_l, in the polystyrene film at the crest of a wrinkle assuming simple bending:

$$\varepsilon_l \sim \left(\frac{t}{2\lambda}\right)\left(\frac{A_w}{\lambda}\right) \sim \left(\frac{3E_s}{8E_f}\right)^{2/3}\varepsilon^{1/2}. \quad (7)$$

For the average applied strain at which folding is observed ($\varepsilon \sim 0.03$), the local strain, ε_d, equals 0.0004. The yield strain for bulk PS is approximately 0.01,[25] which is significantly higher than the local maximum strain calculated for our wrinkling system just prior to folding. Thus, we do not believe plastic deformation induces folding in our materials, but rather folding is a non-linear elastic transition similar to previous reports.[12,22]

5 Conclusions

In this paper, we discussed the wrinkle to strain localization transition of a glassy polymer film placed on an elastomeric substrate. The amplitude of the strain localized features was analyzed both locally and globally. Local analysis showed that wrinkling amplitude increased with applied strain, following the classical wrinkling theory until strain localizations occurred. Delamination amplitude jumped spontaneously and decreased the wrinkling amplitude nearby; whereas, folding amplitude slowly deviated from wrinkling amplitude. Statistically, it was shown that the wrinkling exhibits a distribution of amplitudes. As folding occurred, the wrinkling distribution widened, and delamination caused multiple wrinkling peaks. A critical strain deformation mode map was constructed, and it was found that

delamination was preferred for thick films; whereas, folding was observed prior to delamination for thin films. Importantly, the observed folds grow away from the substrate, in contrast to previous observations of strain localizations growing into the substrates.

Acknowledgements

The funding for this work was provided by NSF DMR-0907219, NSF MRSEC (NSF DMR-0820506), and EPSCoR (EPS-0814442). The authors would like to thank Professor John W. Hutchinson for helpful discussions. Y. E. would like to thank Jonathan Pham for the help with the atomic force microscope.

References

1 A. Lobkovsky, S. Gentges, H. Li, D. Morse and T. A. Witten, *Science*, 1995, **270**, 1482–1485.
2 Z. Y. Huang, W. Hong and Z. Suo, *J. Mech. Phys. Solids*, 2005, **53**, 2101–2118.
3 D. G. Roddeman, J. Drukker, C. W. J. Oomen and J. D. Janssen, *J. Appl. Mech.*, 1987, **54**, 884–887.
4 K. Lu, M. Accorsi and J. Leonard, *Int. J. Numer. Methods Eng.*, 2001, 1017–1038.
5 E. P. Chan and A. J. Crosby, *Soft Matter*, 2006, **2**, 324–328.
6 N. Bowden, W. T. S. Huck, K. E. Paul and G. M. Whitesides, *Appl. Phys. Lett.*, 1999, **75**, 2557–2559.
7 E. P. Chan, E. J. Smith, R. C. Hayward and A. J. Crosby, *Adv. Mater.*, 2008, **20**, 711–716.
8 S. P. Lacour, S. Wagner, Z. Y. Huang and Z. Suo, *Appl. Phys. Lett.*, 2003, **82**, 2404–2406.
9 C. M. Stafford, C. Harrison, K. L. Beers, A. Karim, E. J. Amis, M. R. VanLandingham, H. Kim, W. Volksen, R. D. Miller and E. E. Simony, *Nat. Mater.*, 2004, **3**, 545–550.
10 T. Ohzono and M. Shimomura, *Phys. Rev. B: Condens. Matter Mater. Phys.*, 2004, **69**, 132202.
11 H. G. Allen, *Analysis and Design of Structural Sandwich Panels*, Pergamon Press, New York, NY, 1969, pp. 178–283.
12 L. Pocivavsek, R. Dellsy, A. Kern, S. Johnson, B. Lin, K. Y. C. Lee and E. Cerda, *Science*, 2008, **320**, 912–916.
13 R. Machemer, *Br. J. Ophthalmol.*, 1978, **62**, 737–747.
14 D. P. Khang, J. A. Rogers and H. H. Lee, *Adv. Funct. Mater.*, 2009, **19**, 1526–1536.
15 K. Efimenko, M. Rackaitis, E. Manias, A. Vaziri, L. Mahadevan and J. Genzer, *Nat. Mater.*, 2005, **4**, 293–297.
16 D. P. Holmes and A. J. Crosby, *Phys. Rev. Lett.*, 2010, **105**, 1–4.
17 T. Boatwright, A. J. Levine and M. Dennin, *Langmuir*, 2010, **26**, 12755–12760.
18 H. Diamant and T. W. Witten, *Phys. Rev. Lett.*, 2011, **107**, 164302.
19 J. Genzer and J. Groenewold, *Soft Matter*, 2006, **2**, 310–323.
20 C. Harrison, C. M. Stafford, W. Zhang and A. Karim, *Phys. Rev. Lett.*, 2004, **85**, 4016–4018.
21 L. Pocivavsek, B. Leahy, N. Holten-Anderson, B. Lin, K. Y. C. Lee and E. Cerda, *Soft Matter*, 2009, **5**, 1963–1968.
22 A. B. Croll and A. J. Crosby, *Macromolecules*, 2012, **45**, 4001–4006.
23 D. Vella, J. Bico, A. Boudaoud, B. Roman and P. M. Reis, *Proc. Natl. Acad. Sci. U. S. A.*, 2009, **106**, 10901–10906.
24 J. Zhang, X. Zhao, Y. Cao and J. W. Hutchinson, *J. Mech. Phys. Solids*, 2012, **60**, 1265–1279.
25 R. Quinson, J. Perez, M. Rink and A. Pavan, *J. Mater. Sci.*, 1997, **32**, 1371–1379.